Nano Energy 36 (2017) 206–212

Contents lists available at ScienceDirect

Nano Energy

journal homepage: www.elsevier.com/locate/nanoen

Full paper

Novel conductive binder for high-performance silicon anodes in lithium ion batteries

Dong Liu[a,b,1], Yan Zhao[a,1], Rui Tan[a,1], Lei-Lei Tian[a], Yidong Liu[a], Haibiao Chen[a], Feng Pan[a,*]

[a] School of Advanced Materials, Peking University, Shenzhen Graduate School, Shenzhen 518055, People's Republic of China
[b] BUCT-CWRU International Joint Laboratory, College of Energy, Beijing University of Chemical Technology, Beijing 100029, People's Republic of China

ARTICLE INFO

Keywords:
Water-soluble polymer
Multiple-carboxyl
Conductive binder
Silicon anodes
Lithium ion batteries

ABSTRACT

A novel polymer is designed to serve as the conductive binder for high-capacity silicon anodes in lithium ion batteries (LIBs), aiming to address fast capacity fade and poor cycle life of silicon anodes caused by large volume change during repeated cycles. Abundant carboxyl groups in the polymer chain can effectively enhance the binding force to Si nanoparticles (NPs) and the n-type polyfluorene backbones of the polymer significantly promote the electronic conductivity under the reducing environment for anodes, dual-features of which can maintain electronic integrity during lithiation/delithiation cycles. Notably, the polymer can react with the polar groups on the surface of Si NPs to form strong chemical bonds, thus truly maintaining the electrode mechanical integrity and good electronic conductivity after repeated charge/discharge process. The as-assembled batteries based on the polymer without any conductive additive exhibit a high reversible capacity (2806 mA h g^{-1} at 420 mA g^{-1}) and good cycle stability (85.2% retention of the initial capacity) after 100 cycles.

1. Introduction

Lithium ion batteries (LIBs) are widely used in portable electronic products, however, there are still some concerns for their applications in electric vehicles and renewable energy storage grids, including energy density, cost, and safety [1–4]. Therefore, development of LIBs with high energy density and long cycle life is extremely important. Enormous efforts have been focused on high capacity silicon anodes for increasing energy density of LIBs. Silicon anodes possess a high theoretical capacity (ca. 4200 mA h g^{-1}), which is about ten times higher than that of the currently available commercial graphite anodes (ca. 370 mA h g^{-1}). However, fast capacity fade and poor cycling stability of Si anodes caused by volume expansion (400%) and shrinkage during repetitive lithiation and delithiation cycles have seriously restricted the application of Si anodes in high energy LIBs [5].

Tremendous efforts have been devoted to addressing the above mentioned problem of silicon anodes, by preparing nanostructured Si [6,7], controlling voltage [8,9], and using novel binder [10–12]. For nanoscale Si anodes, the main issue is that Si NPs easily lose electronic connection during cycling because the conductive additive has no mechanical binding force with the active materials. The cycling performance of nanoscale Si anodes can be easily improved by using high performance binders, including carboxymethylcellulose sodium (CMCNa) [10], alginate [11], poly(acrylic acid) (PAA) [12], styrene butadiene rubber (SBR) [13], dopamine modified alginate [14], gum arabic [15], hyperbranched β-cyclodextrin polymer [16], guar gum [17], polyimide [18], polysaccharide [19]. Compared with conventional polyvinylidene fluoride (PVDF) binder, these polymeric binders possess higher Young's moduli and higher contents of functional groups, such as hydroxyl, carboxyl and catechol. These functional groups can increase the binding force between the binder and Si surface, and significantly improve the cycle stability of silicon anodes. Besides novel binders, cross-linked reaction [20,21], host-guest chemistry [22] and self-healing chemistry [23] were also used for improving the cyclic performance of silicon anodes.

In conventional approach, the electrode consists of three components which include active material, conductive additive and polymeric binder. But use of both conductive additive and binder significantly reduces the volumetric and gravimetric capacity of the electrode. Liu et al. [24] first reported a novel conductive polymer as a bi-functional binder instead of separate conductive additive and conventional binder. They found that Si anodes based on this conducting polymer without any conductive additive showed high capacity and excellent cycling performance. Afterwards, other conductive polymers including poly(2,7-9,9-dioctylfluorene-2,7-9,9-(di(oxy-2,5,8-trioxadecane))fluorene-*co*-2,7-fluorenone-*co*-2,5-1-methybenzoate ester) (PFEM) [25]

* Corresponding author.
E-mail address: panfeng@pkusz.edu.cn (F. Pan).
[1] These authors contributed equally to this work.

http://dx.doi.org/10.1016/j.nanoen.2017.04.043
Received 4 March 2017; Received in revised form 20 April 2017; Accepted 20 April 2017
Available online 21 April 2017

and poly(1-pyrenemethyl methacrylate-*co*-triethylene oxide methyl ether methacrylate) (PPyE) [26] were reported. Furthermore, polyaniline (PANI) hydrogels [27], poly(phenanthrenequinone) (PPQ) [28], poly(3,4-ethylenedioxythiophene):poly(styrenesulfonate) (PEDOT:PSS) [29,30], and conductive gels [31] were also used as binders for improving the cycling performance of Si based anodes. In comparison with three-component electrode systems, these two-component electrode systems based on conducting polymeric binders can increase the volumetric capacity of Si anodes via decreasing the proportion of high specific area and inactive conductive additive in the electrodes. More importantly, conductive binders combine the functionality of both binder and conductive additive, avoiding the use of nonconductive binders. Thus, the electrical connectivity problem of the Si electrode is mitigated and the cycling performance is noticeably improved because of its good flexibility and mechanical property. Although considerable progress has been achieved in conducting polymeric binder, developing novel conducting polymeric binders for high capacity silicon anodes remains a challenge.

Conventional water-soluble binders (such as CMC-Na) significantly improve the electrochemical performance owing to their favorable interactions with the surface of Si NPs. But their insulating nature leads to poor electrical connections mainly because the conductive additive tends to be pushed away from Si NPs due to huge volume expansion of Si anodes during charging (Fig. 1a). Herein, we report a water-soluble multiple-carboxyl polymer as a conductive binder for improving the electrochemical performance of the silicon anodes. The polymer consists of an n-type polyfluorene backbones and abundant carboxyl functional groups on the side chains. The polymeric binder shows excellent thermal stability due to its extremely simple structural design. In addition, the polymer backbone can be cathodically doped for enhanced electronic conductivity under the reducing environment for anodes. Abundant carboxyl groups on the side chains can considerably enhance adhesion force and electrolyte absorption. These properties are essential for an outstanding conductive binder. More importantly, these carboxylic sodium groups can react with the hydroxyl groups of SiO_2 on the surface of Si NPs, yielding new chemical bonds between silicon and binder. This can ensure constant electrical connections even as the Si particles disintegrate into pieces (Fig. 1b). Thus, this novel polymer can endure dramatic volume changes of active Si to achieve high capacity and excellent cycle life, which was demonstrated in as-assembled batteries using the polymeric binder.

2. Material and methods

2.1. Synthesis of conductive polymers

2.1.1. Synthesis of poly(2,7–9,9-dioctylfluorene) (PFO)

A mixture containing 0.548 g (1 mmol) of 2,7-Dibromo-9,9-di-n-octylfluorene, 0.558 g of (1 mmol) 9,9-dioctylfluorene-2,7-diboronic acid bis(1,3-propanediol) ester and several drops of Aliquat 336 in 13 mL of THF and 5 mL of 2 M Na_2CO_3 solution was added into a Schlenk flask. The flask was degassed by three freeze–pump–thaw cycles, and then 0.057 g of $[Pd(PPh_3)_4]$ was added quickly and refluxed with vigorous stirring for 72 h under a nitrogen atmosphere. After the

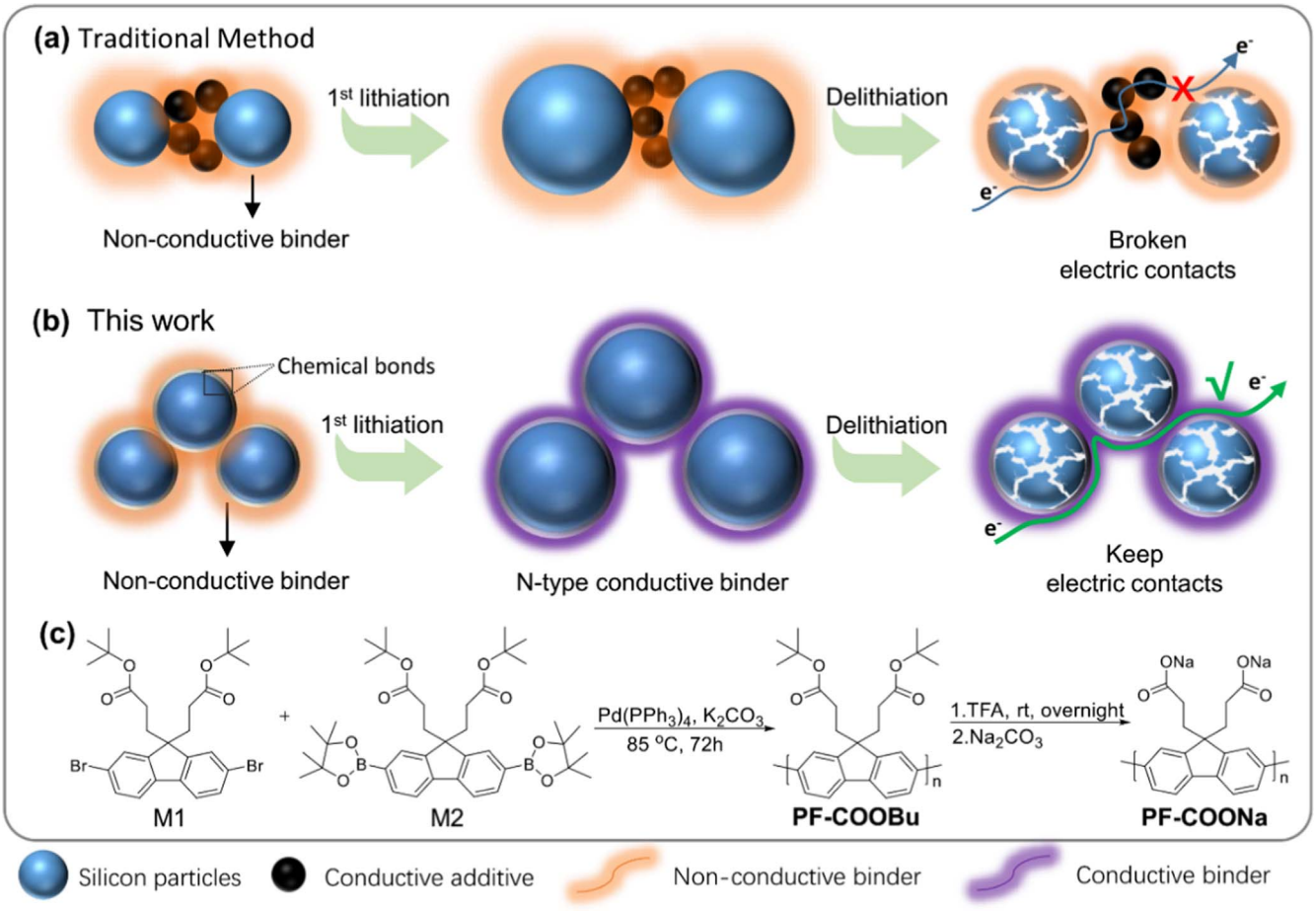

Fig. 1. Schematics of the approaches to address volume change issue in battery materials. (a) Traditional approaches using acetylene black (AB) as the conductive and non-conductive polymer as mechanical binder. (b) Replacing conductive additive and non-conductive binder, conductive binder could keep the electrical and mechanical integrity of the electrode during repeated charge/discharge cycles. (c) Synthetic scheme of the novel conductive polymer sodium poly(3,3′-(9H-fluorene-9,9-diyl)dipropionic acid) abbreviated as PF-COONa.

mixture was cooled down, the polymer was precipitated from methanol three times, filtered and dried under vacuum, obtaining the final polymer with a 79% yield. ^{1}H NMR (400 MHz, $CDCl_3$) δ (ppm): 7.87–7.69 (br, 6H); 2.13 (br, 4H); 1.15 (br, 24H); 0.83 (m, 12H). ^{13}C NMR (400 MHz, $CDCl_3$), δ(ppm): 151.8, 140.5, 126.1, 121.5, 119.9, 55.3, 40.4, 31.8, 30.0, 29.2, 23.9, 22.6, 14.0. GPC (THF, PS standard): Mn=8800, PDI=2.8.

2.1.2. Synthesis of poly[9,9-bis(3-tert-butyl propanoate)fluorine] (PF-COOBu)

A mixture of 0.582 g of 2,7-Dibromo-9,9-bis(3-tert-butyl propanoate)fluorine (1 mmol), 0.680 g of 2,7-bis(4,4,5,5-tetrameth-yl-1,3,2-dioxaborolan-2-yl)-9,9-bis(3-tert-butyl ropanoate)fluorine (1 mmol), several drops of Aliquat 336 in 13 mL of THF, and 5 mL of 2 M Na_2CO_3 solution was added into a Schlenk flask. The flask was degassed by three freeze–pump–thaw cycles, and then $[Pd(PPh_3)_4]$ (0.057 g) was added quickly and refluxed with vigorous stirring for 72 h under a nitrogen atmosphere. After the mixture was cooled down, the polymer was precipitated from methanol three times, filtered and dried under vacuum, obtaining the final polymer with an 85% yield. ^{1}H NMR (400 MHz, $CDCl_3$) δ (ppm): 7.87–7.87 (br, 6H); 2.54 (br, 4H); 1.65 (br, 4H); 1.32 (s, 18H). ^{13}C NMR (400 MHz, $CDCl_3$), δ(ppm):172.8, 149.2, 140.6, 140.2, 127.0, 121.6, 120.4, 80.1, 54.0, 34.7, 30.1, 28.0. GPC ($CHCl_3$, PS standard): Mn=4100, PDI=1.85.

2.1.3. Synthesis of sodium poly[9,9-bis(3-propanoate)fluorine] (PF-COONa)

500 mg of PF-COOBu was dissolved in 300 mL dichloromethane. Subsequently, 30 mL trifluoroacetic acid was added to the solution. The mixture was stirred overnight at room temperature. After the reaction stopped, the solvent was removed under reduced pressure, yielding a yellowish-green residue. The residue was treated with 100 mL 0.05 M aqueous Na_2CO_3 solution and purified by dialysis against water for 3 days. The purified solution was freeze-dried to give PF-COONa with a 67% yield. 1H NMR (400 MHz, $CDCl_3$) δ (ppm): 7.92–7.76 (br, 6H); 2.45 (br, 4H); 1.45 (br, 4H).

2.2. Material characterizations

Fourier transform infrared (FTIR) spectra were collected on a Nicolet Avatar 360 spectrophotometer (KBr tablet). Nuclei magnetic resonance (NMR) spectrometers (^{1}H NMR and ^{13}C NMR) were recorded on a Bruker DPX 400 MHz spectrometers. Number average molecule weight (Mn) and polydispersity index (PDI) was determined by GPC (Waters 515-2410 system). X-ray photoelectron spectra (XPS) of samples were collected by using ESCALAB 250Xi. Thermogravimetric analysis (TGA) was carried out with a Seiko Exstar 6000 instrument at a scanning rate of 10 °C min^{-1} under nitrogen atmosphere.

2.3. Electrochemical measurements

All electrodes based on as-synthesized polymers were prepared using casting method. Firstly, 60 mg of PF-COONa was dispersed in 1 mL deionized water through stirring for 6 h. Then a defined amount of Si nanoparticles was homogeneously dispersed into PF-COONa aqueous solution with the desired Si to polymer weight ratios. Working electrodes were prepared by spreading the above slurry onto a Cu foil (thickness=20 μm) current collector. The electrodes were dried at 135 °C under vacuum for removing H_2O molecules. The mass ratio of Si/binder was the same (66.6:33.3) in this article and different ratio of Si/PF-COONa electrodes had been mentioned in the manuscript. The electrode based on PFO were preparing by using the same procedure. The solvent for dissolving PFO was THF. The electrolyte for all tests consisted of 1.2 M $LiPF_6$ in ethylene carbonate (EC) and diethylene carbonate (DEC) (1:1 w/w) with 30 wt% fluoroethylene carbonate (FEC). All coin cells were assembled in an Ar-filled glovebox.

The electrochemical measurements were conducted by galvanostatic cycling of 2032-type coin half cells using Li foil (99.9%, China Energy Lithium Co. Ltd, Tianjin) as the counter electrodes. Galvanostatic charge/discharge measurement was conducted over a voltage range of 0.01–1 V at room temperature by Neware battery test system (Newell, China). The cyclic voltammetry (CV) measurements were carried out using electrochemical workstation (CHI 604E) at a scan rate of 0.2 mV s^{-1} in the voltage range of 0.01–3 V (vs Li/Li$^+$). The electrochemical impedance spectroscopy (EIS) experiments were performed on an electrochemical workstation (CHI 660E) in the frequency range of 10 Hz to 1 MHz.

3. Results and discussion

The synthesis of the novel conductive polymer (sodium poly(3,3′-(9H-fluorene-9,9-diyl)dipropionic acid) denoted as PF-COONa) is schematically illustrated in Fig. 1c, where the monomers of M1 and M2 were synthesized according to the previous reports (The details are shown in Supporting Information) [32–34]. The condensation polymerization of these monomers was completed by using the Suzuki coupling reaction, after which the obtained polymer (PF-COOBu) was acid-hydrolyzed and subsequently neutralized by extra sodium carbonate to gain the water-soluble PF-COONa. The designed polymer with expected advantages possesses a polyfluorene type backbone and masses of propanoate sodium side chains. When used as a binder, this binder with stable chemical properties exhibits little-to-no interaction with electrolyte solvent. Notably, the strength of adhesion force can be dramatically promoted through the interaction between the carboxyl groups of the binder and the hydroxyl groups on the surface of Si-based materials.

The TEM image of the raw Si particles shows the average size is about 50 nm (Fig. S1a). And the high-magnification TEM image demonstrates the existence of about 5 nm Si oxide components on the surface of the Si particles (Fig. S1b). Fourier transform infrared (FTIR) spectroscopy studies provide more details of the content of oxygen of the raw Si. The raw Si film exhibits a peak at ~1207 cm^{-1} related to Si-O-Si antisymmetric vibrations, a peak at ~1134 cm^{-1} related to Si-O-Si symmetric vibrations and a peak around 3449 cm^{-1} corresponds to hydrogen-bonded O-H stretching vibrations. These results show that silicon particles are covered by SiO_2 layers [35], and abundant hydroxyl groups exist on the surface of SiO_2 layer. Previous studies suggest that the presence of these free polar groups on the Si-based materials contributes to the cycling performance of Si-based anode due to their interaction with water-soluble binder [36–38]. When the binder is mixed with Si nano-particles, the -COONa group partially hydrolyzes to form -COOH group and then react with the -OH groups on the silicon surface to yield an ester –C=O–OR bond [36,39]. The chemical bonds between the carboxylic groups and the hydroxyl groups of the Si NPs can be directly identified by Fourier Transform Infrared (FTIR) spectroscopy (Fig. 2a and Fig. S2). In a typical FTIR spectrum of the binder PF-COONa (Fig. S2), the peaks located at 2921 cm^{-1} and 1458 cm^{-1} respectively correspond to the stretching vibration and bending vibration of C–H bond on the side chains. Two strong bands at 1560 cm^{-1} and 1407 cm^{-1} are ascribed to asymmetric and symmetric stretching vibrations of the carboxylic acid salt –COO$^-$ of PF-COONa [9,11,15]. Besides, it is obviously observed that two characteristic absorption peaks belonging to the carboxylic acid salt are greatly weakened, and even disappeared when PF-COONa is mixed with Si particles in the slurry and treated at 135 °C for 12 h. A new but sharp band around 1704 cm^{-1} corresponding to the stretching vibration of carbonyl group appears, indicating the formation of new chemical bonds CO–OR between the polymer and Si particles (Fig. 2a) [20,21]. This result demonstrates that the conductive binder can be reacted with SiO_2 of the Si NPs surface through strong chemical interaction. To further prove that Si NPs can be chemically bonded

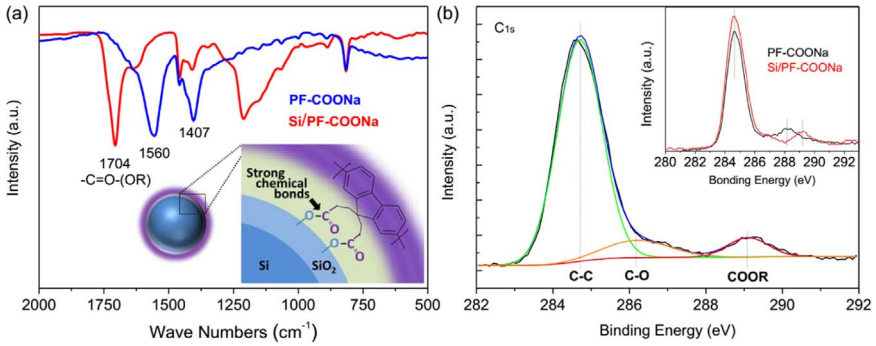

Fig. 2. (a) FT-IR spectra of the polymer PF-COONa and Si/PF-COONa electrode (inset is the schematic of the formation of chemical bonds between PF-COONa and Si particle). (b) XPS spectra of Si/PF-COONa electrode (inset is the XPS spectra comparison between pure PF-COONa binder and Si/PF-COONa electrode).

with PF-COONa, the electrode plates consisting of Si/PF-COONa composites were dried at 135 °C in the vacuum oven for 12 h. Then electrode plates are washed by plenty of deionized water in order to remove free PF-COONa molecules. Whereafter, the above products were dried for the second time and then analyzed by X-Ray Photoelectron Spectroscopy (XPS). The C1s XPS spectra of the PF-COONa and Si/PF-COONa composites shown in Fig. 2b reveal the formation of strong chemical bonds between the PF-COONa binder and the polar surface of Si particles. The pristine PF-COONa shows a clear peak corresponding to –COONa functional groups at 288.2 eV. However, the peak is greatly weakened and an additional peak corresponding to –C=O–(OR) at 289.1 eV is observed after mixing PF-COONa with Si NPs (Fig. 2b). After an extensive cleaning of the composite, the peak at 288.2 eV disappears and the peak at 289.1 eV is still retained, indicating that most free polymer molecules were removed while polymer molecules strongly bonded to the SiO_2 surface of Si NPs remained intact (Fig. S3). These results match well with the conclusion of FTIR studies, suggesting there are strong chemical interactions between the polar groups on the silicon surface and PF-COONa moieties.

In addition to abundant polar functional groups contributing to the strong interactions between the binder and Si particles, the polymeric binder provides an n-type doped polyfluorene, which can be cathodically doped under the reducing environment for anodes. To measure the electrochemical properties of pure PF-COONa, cyclic voltammetry was conducted at a scanning rate of 0.2 mV s^{-1} between 0.01 and 3.0 V (versus Li/Li^+) as shown in Fig. 3a. The differential capacity curves show two cathodic peaks indicating the first cathodical doping at 1.5 V, and the second around 0.75 V. This result is similar to previous reports [24]. Furthermore, the following cycles except for the first one provide good reproducibility with excellent overlapping of all the peaks, suggesting stable electrochemical process. Analogous results are observed in the CV curve of PFO without any active functional groups on the side chains (Fig. S4). These results demonstrate that PF block chains rather than side chains can provide reversible electrochemical activity. Fig. S5 shows the charge/discharge voltage curves of pure PF-COONa electrode at a low current density of 20 mA g^{-1} over the potential window of 0.01–3.0 V. Typically, two lithiation/delithiation processes are observed, which is consistent with the results of CV. The first discharge specific capacity of the PF-COONa electrode without any conductive additive is 60.5 mA h g^{-1}, and a reversible capacity of 43.4 mA h g^{-1} remains after 100 cycles at a current density of 20 mA g^{-1}, suggesting PF-COONa binder can withstand repeated n-doping/de-doping process in the potential window of 0.01–3 V versus Li/Li^+ (Fig. S6). Due to the n-type doping on the PF backbone, improved electronic conductivity can be experimentally verified by the impedance measurements (Fig. 3b). In fact, it's clearly observed that both doping happening around 1.5 V and 0.75 V enhance the electronic conductivity, which is increased by one time when doping potential changes from 1 V to 0.01 V (Fig. 3b). This is a potential window that can fulfill the operation of Si based anodes.

The adhesion ability of the binder is a pivotal factor for Li-ion batteries. Poor adhesion of binders leads to delamination of active materials from the current collector and subsequently causes fast capacity fading during repeated charge/discharge cycles. Thus, besides a strong interaction with the surface of Si particles, an ideal polymeric binder should provide superior mechanical adhesion force between the active material and the current collector. Adhesive properties of composite electrodes were evaluated by widely adopted peeling tests, and more details are presented in the Supporting Information. As shown in Fig. 3c, Si/PF-COONa electrodes exhibit the highest average peeling force at about 6.6 N, which is slightly higher than that of CMC-Na/AB/Si electrodes, suggesting that the polymer can effectively adhere on the polar surface of Si particles and the copper oxide (CuO) surface of the Cu current collector. Another polyfluorene type polymer PFO without any polar functional groups was synthesized and the peeling test just show a peeling force of 2.7 N, which was much lower than that of polar binders, suggesting that adhesion of the polar binder was enhanced by abundant –COONa groups. These results demonstrate that the substantial polar functional groups of the polymer offer the excellent adhesion, potentially improving the mechanical stability of actual electrodes. In addition, an efficient Li-ion ionic conductivity is beneficial for extracting the entire capacity of the active material. The polymer coating on the surface of the active materials may have a great influence on the Li^+ transportation efficiency at the interface between the active material and the polymeric binder. Sufficient electrolyte absorption is critical for allowing Li^+ diffusion to the active material and subsequently achieving high capacity and improved rate performance of Si-based electrodes. The swelling ability of polymeric binders was measured in electrolyte at room temperature (shown in Fig. 3d). In the polyfluorene type binder system, PF-COONa shows a high electrolyte uptake up to 47% of its initial weight in 30 h, which is much higher than the electrolyte uptake by PFO (about 5 wt%).

The thermal stability for PF-COONa binder was evaluated by thermogravimetric analysis (TGA) to determine the water content and the decomposition temperature. The TGA results reveal that the polymer PF-COONa contains 15.5 wt% crystal water. And the steep curve shows excellent thermal stability in which case the initial decomposition temperature is about 301 °C (Fig. S7), revealing that the polymeric binder can be utilized in a wide temperature range. Furthermore, 6 wt% PF-COONa aqueous solution is applied to prepare the Si/PF-COONa electrode. The pH of the solution is just about 8, suggesting the Si or SiO_2 layer can keep stable under such a weak alkaline condition. Thus, PF-COONa is quite suitable to be a water-soluble binder for Si anodes.

The electrochemical performances of Si/PF-COONa electrode are shown in Fig. 4. Fig. 4a presents the first five cyclic voltammetry (CV) curves of a typical Si-based electrode at a sweep rate of 0.2 mV s^{-1}. The cathodic peak at 0.25 V on the first CV curve is ascribed to the

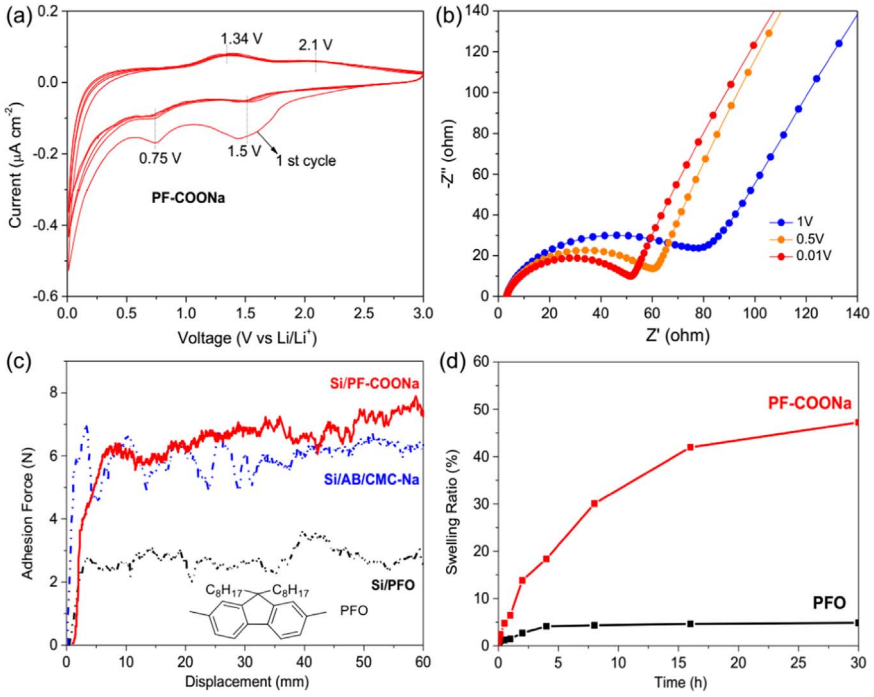

Fig. 3. (a) Cyclic voltammogram of PF-COONa electrode between 0.01 and 3.0 V (vs Li/Li+) at 0.2 mV s^{-1} at room temperature. (b) Enhanced conductivity of pure PF-COONa polymer at different potentials, (c) adhesion force of the Si/PF-COONa, Si/AB/CMCNa, and Si/PFO electrodes, (inset is the structure of polymer PFO). (d) Swelling tests of PF-COONa and PFO polymer films in the electrolyte.

formation of solid electrolyte interface layer on the polar surface of the Si electrode. The formation of Li-Si alloy begins at ~0.33 V and decreases rapidly below 0.2 V, which corresponds to the formation of different alloy phases of $Li_{12}Si_7$ and $Li_{15}Si_4$, respectively. The delithiation curve shows two cathodic peaks around 0.35 V and 0.55 V, corresponding to the transformation of amorphous Li_xSi to Si phase. The increase of charge-discharge current with cycling is attributed to a gradual activation of more active Si NPs embedded in the thick electrode. The CV results are consistent with the previous reports [40]. Fig. 4b shows the typical charge-discharge curves of Si/PF-COONa electrode at a constant current density of 420 mA g^{-1}. The first discharge curve presents a long plateau, suggesting crystalline Si reacts with lithium to form amorphous Li_xSi. The first discharge capacity is 4396 mA h g^{-1} (based on the mass of Si), corresponding to a coulombic efficiency of 68.4%. The subsequent charge/discharge cycles show different characteristic voltage profiles, which is ascribed to

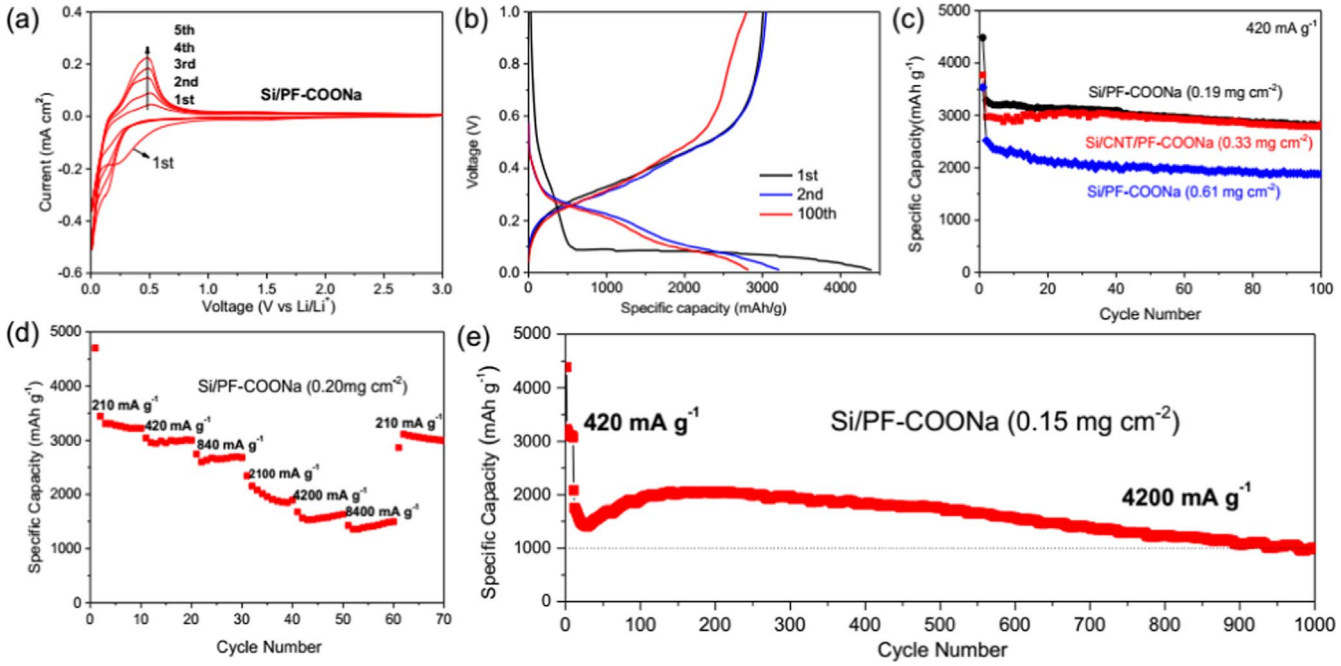

Fig. 4. Electrochemical performances of Si-based electrodes. (a) a typical C-V profile of the Si/PF-COONa electrode at a scanning rate of 0.2 mV s^{-1} between 0.01 and 3.0 V (vs Li/Li^+) (b) 1st, 2nd and 100th cycle curves of Si/PF-COONa electrode at a current density of 420 mA g^{-1}. (c) Cycling performances of Si/PF-COONa, Si/CNT/PF-COONa and high-load Si/PF-COONa electrodes between a cycling voltage of 0.01 and 1 V for 100 cycles at a current density of 420 mA g^{-1}. (d) Rate performance of Si/PF-COONa electrode at current density of 210, 420, 840, 2100, 4200, 8400 mA g^{-1}. (e) Long cycling performance of Si/PF-COONa electrode at a high current rate of 4200 mA g^{-1}.

the formation of amorphous Li_xSi and Si, respectively. The second cycle exhibits a capacity of 3215 mA h g^{-1} with a high columbic efficiency of 94.7%. High specific capacity and columbic efficiency remain in the following cycles, indicating a good cycling stability of Si/PF-COONa electrode.

Fig. 4c shows the cycling performance of Si/PF-COONa electrode measured at a current density of 420 mA g^{-1}. All current density and specific capacity are based on the mass of active Si. A high irreversible capacity loss is observed, which is mainly ascribed to the expected side reaction. In the side reaction, solvent molecules and salt anions were reduced to form insoluble Li salt on the active material surface, forming precipitated solid electrolyte interface (SEI) [15]. The SEM images in the Fig. S8 demonstrate the typical morphology before and after cycling. The formation of solid electrolyte interface on the Si/PF-COONa electrode (Fig. S8b) could attribute to the stability during the subsequent cycling. The cycling curves in the Fig. 4c show that the first reversible specific capacity of Si/PF-COONa electrode is as high as 3291 mA g^{-1} close to the theoretical capacity of Si. After the first two cycles, the coulombic efficiency rapidly increases and remains highly stable during the subsequent cycling, suggesting excellent reversible cycling performance. The reversible specific capacity after 100 cycles at a current density of 420 mA g^{-1} is 2806 mA h g^{-1}, which corresponds to 85.2% retention of the initial capacity when the loading of Si was 0.19 mg cm^{-2}. When the loading of Si was increased to 0.61 mg cm^{-2} in the Si/PF-COONa electrode without any conductive additive, the electrode still shows a reversible specific capacity of 2521 mA h g^{-1} and maintains 84% of its initial capacity at a current density of 420 mA g^{-1} even after 100 cycles. To further evaluate the PF-COONa as a novel binder, the electrochemical performance of Si/carbon nanotube (CNT)/PF-COONa electrode is compared. It's observed that the electrode deliver a reversible specific capacity of 2824 mA h g^{-1} after 100 cycles, which corresponds to 95.1% retention of the initial capacity. The cycle stability of the Si electrodes can be further increased by added CNTs into electrodes.

In addition, the electrode also displayed good rate capability indicating the excellent conductivity of Si/PF-COONa electrode. As shown in Fig. 4d, the electrode was able to preserve reversible specific capacities of 3433, 3043, 2742, 2344, 1678, and 1424 mA h g^{-1} at current densities of 210, 420, 840, 2100, 4200 and 8400 mA g^{-1}, respectively. Furthermore, through multiple rate cycles, the reversible capacity of Si/PF-COONa electrode was able to regain back to 3113 mA h g^{-1} at a current density of 210 mA g^{-1}, suggesting excellent mechanical stability contributing to cycling performance at high current density. Fig. 4e shows the long-term cycling performance at a current density of 4200 mA g^{-1}. It can be seen that a specific capacity of 999 mA h g^{-1} is retained after 1000 cycles, which is quite high for pure Si based electrode without any conductive additive, indicating good electronic conduction and mechanical integrity.

The electrochemical performance of Si/PF-COONa electrodes with different binder contents are shown in Fig. S9. The electrode with 33.3% conductive binder provides the best cycling stability, and the ratio is consistent with previous reports about Si/conductive binders [24]. This result suggests that higher conductive binder content can enhance the mechanical strength of the electrode and contribute to improvement of long-term cycling. Compared with other published conductive binders as shown on the Table S1, this novel conductive binder displays superior comprehensive performance due to its unique design of multiple-carboxyl polymer. To further demonstrate the advantage of this water-soluble conductive binder, the electrochemical performances of Si/CMC-Na and Si/AB/CMC-Na electrodes are compared with Si/PF-COONa electrode (Fig. S10). The Si/CMC-Na and Si/AB/CMC-Na electrodes are characterized by high starting capacity but fast capacity fading, ascribing to the insulating nature of sodium carboxymethylcellulose (CMC-Na) and the loss of electrical integrity. With the designed electronic mechanical properties, PF-COONa achieves high specific capacity and stable cycling performance. This finding suggests that this water-soluble conductive binder possesses larger advantages than traditional water-soluble binders, indicating great potential for commercial applications as a novel anode binder.

4. Conclusion

In summary, an additive-free Si electrode based on a novel water-soluble conductive binder demonstrated high capacity and long cycle stability. The excellent performance of the Si/PF-COONa electrode is mainly attributed to the unique structure design of PF-COONa. The polymeric binder provides abundant carboxyl groups on the side chains for increasing the binding force, and n-type polyfluorene backbones contributing to the improvement of the electronic conductivity. Due to the formation of chemical bonds between the polymeric binder and the polar groups on the Si particle surface, the electrode can endure dramatic volume changes of Si and maintain electronic integrity during repeated charge/discharge cycles. Si anodes using this novel polymeric binder without any conductive additive showed a reversible capacity of 2806 mA h g^{-1} at 420 mA g^{-1} after 100 cycles (85.2% retention of the initial capacity). Even under a rate current of 4.2 A g^{-1}, the specific capacity can still maintain 999 mA h g^{-1} over 1000 cycles of charge and discharge. Furthermore, the polymeric binder provides good thermal stability, benign compatibility with the electrolyte and low cost, indicating great potential for commercial applications as a novel water-soluble binder.

Acknowledgements

D.L., Y.Z. and R.T. contributed equally to this work. The research was financially supported by Chinese Postdoctoral Science Foundation (No. 2015M570894), Shenzhen Science and Technology Research Grant (No. JCYJ20150629144453251), Guangdong Innovation Team Project (No. 2013N080), Shenzhen Science and Technology Research Grant (peacock plan KYPT20141016105435850), and National Materials Genome Project (2016YFB0700600).

Appendix A. Supplementary material

Supplementary data associated with this article can be found in the online version at doi:10.1016/j.nanoen.2017.04.043.

References

[1] W.M. Stanley, Chem. Rev. 104 (2004) 4271–4301.
[2] J. Lu, Z.H. Chen, Z.F. Ma, F. Pan, L.A. Curtiss, K. Amine, Nat. Nanotechnol. 11 (2016) 1031–1038.
[3] Y. Wei, J.X. Zheng, S.H. Cui, X.H. Song, Y.T. Su, W.J. Deng, Z.Z. Wu, X.W. Wang, W.D. Wang, M.M. Rao, Y. Lin, C.M. Wang, K. Amine, F. Pan, J. Am. Chem. Soc. 137 (2015) 8364–8367.
[4] J.X. Zheng, T.C. Liu, Z.X. Hu, Y. Wei, X.H. Song, Y. Ren, W.D. Wang, M.M. Rao, Y. Lin, Z.H. Chen, J. Lu, C.M. Wang, K. Amine, F. Pan, J. Am. Chem. Soc. 138 (2016) 13326–13334.
[5] X. Su, Q.L. Wu, J.C. Li, X.C. Xiao, A. Lott, W.Q. Lu, B.W. Sheldon, J. Wu, Adv. Energy Mater. 4 (2014) 1300882.
[6] H. Wu, G. Chan, J.W. Choi, I. Ryu, Y. Yao, M.T. McDowell, S.W. Lee, A. Jackson, Y. Yang, L.B. Hu, Y. Cui, Nat. Nanotechnol. 7 (2012) 309–314.
[7] N. Liu, Z.D. Lu, J. Zhao, M.T. McDowell, H.W. Lee, W.T. Zhao, Y. Cui, Nat. Nanotechnol. 9 (2014) 187–192.
[8] J. Li, J.R. Dahn, J. Electrochem. Soc. 154 (2007) A156–A161.
[9] D. Mazouzi, B. Lestriez, L. Roue, D. Guyomard, Electrochem. Solid State Lett. 12 (2009) A215–A218.
[10] J. Li, R.B. Lewis, J.R. Dahn, Electrochem. Solid State Lett. 10 (2007) A17–A20.
[11] I. Kovalenko, B. Zdyrko, A. Magasinski, B. Hertzberg, Z. Milicev, R. Burtovyy, I. Luzinov, G. Yushin, Science 334 (2011) 75–79.
[12] A. Magasinski, B. Zdyrko, I. Kovalenko, B. Hertzberg, R. Burtovyy, C.F. Huebner, T.F. Fuller, I. Luzinov, G. Yushin, Acs Appl. Mater. Interfaces 2 (2010) 3004–3010.
[13] W.R. Liu, M.H. Yang, H.C. Wu, S.M. Chiao, N.L. Wu, Electrochem. Solid State Lett. 8 (2005) A100–A103.
[14] M.H. Ryou, J. Kim, I. Lee, S. Kim, Y.K. Jeong, S. Hong, J.H. Ryu, T.S. Kim, J.K. Park, H. Lee, J.W. Choi, Adv. Mater. 25 (2013) 1571–1576.

[15] M. Ling, Y.N. Xu, H. Zhao, X.X. Gu, J.X. Qiu, S. Li, M.Y. Wu, X.Y. Song, C. Yan, G. Liu, S.Q. Zhang, Nano Energy 12 (2015) 178–185.
[16] Y.K. Jeong, T.W. Kwon, I. Lee, T.S. Kim, A. Coskun, J.W. Choi, Nano Lett. 14 (2014) 864–870.
[17] J. Liu, Q. Zhang, T. Zhang, J.T. Li, L. Huang, S.G. Sun, Adv. Funct. Mater. 25 (2015) 3599–3605.
[18] J. Choi, K. Kim, J. Jeong, K.Y. Cho, M.H. Ryou, Y.M. Lee, ACS Appl. Mater. Interfaces 7 (2015) 14851–14858.
[19] Y.K. Jeong, T.W. Kwon, I. Lee, T.S. Kim, A. Coskun, J.W. Choi, Energy Environ. Sci. 8 (2015) 1224–1230.
[20] B. Koo, H. Kim, Y. Cho, K.T. Lee, N.S. Choi, J. Cho, Angew. Chem. 51 (2012) 8762–8767.
[21] J.X. Song, M.J. Zhou, R. Yi, T. Xu, M.L. Gordin, D.H. Tang, Z.X. Yu, M. Regula, D.H. Wang, Adv. Funct. Mater. 24 (2014) 5904–5910.
[22] T.W. Kwon, Y.K. Jeong, E. Deniz, S.Y. AlQaradawi, J.W. Choi, A. Coskun, ACS Nano 9 (2015) 11317–11324.
[23] C. Wang, H. Wu, Z. Chen, M.T. McDowell, Y. Cui, Z.A. Bao, Nat. Chem. 5 (2013) 1042–1048.
[24] G. Liu, S.D. Xun, N. Vukmirovic, X.Y. Song, P. Olalde-Velasco, H.H. Zheng, V.S. Battaglia, L.W. Wang, W.L. Yang, Adv. Mater. 23 (2011) 4679–4683.
[25] M.Y. Wu, X.C. Xiao, N. Vukmirovic, S.D. Xun, P.K. Das, X.Y. Song, P. Olalde-Velasco, D.D. Wang, A.Z. Weber, L.W. Wang, V.S. Battaglia, W.L. Yang, G. Liu, J. Am. Chem. Soc. 135 (2013) 12048–12056.
[26] S.J. Park, H. Zhao, G. Ai, C. Wang, X.Y. Song, N. Yuca, V.S. Battaglia, W.L. Yang, G. Liu, J. Am. Chem. Soc. 137 (2015) 2565–2571.
[27] H. Wu, G.H. Yu, L.J. Pan, N.A. Liu, M.T. McDowell, Z.A. Bao, Y. Cui, Nat. Commun. 4 (2013).
[28] S.M. Kim, M.H. Kim, S.Y. Choi, J.G. Lee, J. Jang, J.B. Lee, J.H. Ryu, S.S. Hwang, J.H. Park, K. Shin, Y.G. Kim, S.M. Oh, Energy Environ. Sci. 8 (2015) 1538–1543.
[29] D. Shao, H.X. Zhong, L.Z. Zhang, ChemElectroChem 1 (2014) 1679–1687.
[30] T.M. Higgins, S.H. Park, P.J. King, C. Zhang, N. McEvoy, N.C. Berner, D. Daly, A. Shmeliov, U. Khan, G. Duesberg, V. Nicolosi, J.N. Coleman, Acs Nano 10 (2016) 3702–3713.
[31] X.H. Yu, H.Y. Yang, H.W. Meng, Y.L. Sun, J. Zheng, D.Q. Ma, X.H. Xu, ACS Appl. Mater. Interfaces 7 (2015) 15961–15967.
[32] J. Li, C. Tian, Y. Yuan, Z. Yang, C. Yin, R. Jiang, W. Song, X. Li, X. Lu, L. Zhang, Q. Fan, W. Huang, Macromolecules 48 (2015) 1017–1025.
[33] B. Nowacki, H. Oh, C. Zanlorenzi, H. Jee, A. Baev, P.N. Prasad, L. Akcelrud, Macromolecules 46 (2013) 7158–7165.
[34] P.C. Rodrigues, L.S. Berlim, D. Azevedo, N.C. Saavedra, P.N. Prasad, W.H. Schreiner, T.D. Atvars, L. Akcelrud, J. Phys. Chem. A 116 (2012) 3681–3690.
[35] S. Xun, X. Song, M.E. Grass, D.K. Roseguo, Z. Liu, V.S. Battaglia, G. Liu, Electrochem. Solid State Lett. 14 (2011) A61–A63.
[36] N.S. Hochgatterer, M.R. Schweiger, S. Koller, P.R. Raimann, T. Wöhrle, C. Wurm, M. Winter, Electrochem. Solid State Lett. 11 (2008) A76–A80.
[37] J.S. Bridel, T. Azaïs, M. Morcrette, J.M. Tarascon, D. Larcher, Chem. Mater. 22 (2010) 1229–1241.
[38] H. Zhao, Z. Wang, P. Lu, M. Jiang, F. Shi, X. Song, Z. Zheng, X. Zhou, Y. Fu, G. Abdelbast, X. Xiao, Z. Liu, V.S. Battaglia, K. Zaghib, G. Liu, Nano Lett. 14 (2014) 6704–6710.
[39] N.S. Hochgatterer, M.R. Schweiger, S. Koller, P.R. Raimann, T. Wöhrle, C. Wurm, M. Winter, Electrochem. Solid State Lett. 11 (5) (2008) A76–A80.
[40] B.R. Liu, P. Soares, C. Checkles, Y. Zhao, G.H. Yu, Nano Lett. 13 (2013) 3414–3419.

Dong Liu received his B.Sc. in Polymer Material and Engineering in 2009 and Ph.D. degree in Material Science in 2014 from Beijing University of Chemical and Technology (BUCT). Then he joined Prof. Feng Pan Group as a post-doctoral fellow at School of Advanced Materials, Peking University, Shenzhen Graduate School, China. Now he joins Prof. Liming Dai Group and works at BUCT-CWRU (Case Western Reserve University) International Joint Lab as a post-doctoral fellow. His research interests include energy materials (battery materials, catalytic materials), functional polymers, nanomaterials, and electrochemistry.

Yan Zhao received his B.Sc. degree in 2014 from China Agricultural University, China. He is pursuing his Ph.D. degree in the School of Advanced Materials, Peking University, China. His research interests include advanced functional materials for energy storage and conversion devices, such as conductive polymers, lithium sulfur batteries, all solid-state batteries and so on.

Rui Tan received his B.Sc. degree in 2014 from Central South University, China. He is pursuing his M.Sc. degree in the School of Advanced Materials, Peking University, China. His research interests include advanced functional materials and their new application in energy storage and conversion devices, such as all solid-state batteries, lithium sulfur batteries and so on.

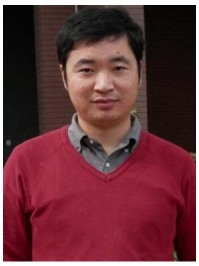

Lei-Lei Tian received his B.Sc. in Materials Science and Engineering in 2009 and Ph.D. degree in Chemical Technology in 2014 from China University of Mining & Technology. Then he joined Prof. Feng Pan Group as a post-doctoral fellow at School of Advanced Materials, Peking University, Shenzhen Graduate School, China. His research interests include energy materials, nanomaterials, and electrochemistry.

Dr. Yidong Liu is currently distinguished researcher in the School of Advanced Materials, Peking University Shenzhen Graduate School. He received his Ph.D. in Chemistry from the Graduate Center/CUNY in 2006. After Ph.D., he worked at Columbia University in the city of New York as an associate research scientist. His research concentrates in high performance materials, composite and devices.

Haibiao Chen is currently a senior researcher at the School of Advanced Materials, Peking University Shenzhen Graduate School. He received his Bachelor's degree from Tsinghua University in 2000 and Ph.D. from Stevens Institute of Technology in 2006. He worked at Velocys during 2006–2011 and UES during 2011–2014 prior to joining Peking University Shenzhen Graduate School.

Prof. Feng Pan, National 1000-plan Professor, Founding Dean of School of Advanced Materials, Peking University Shenzhen Graduate School, Director of National Center of Electric Vehicle Power Battery and Materials for International Research, got B.S. from Dept. Chemistry, Peking University in 1985 and Ph.D. from Dept. of P & A Chemistry, University of Strathclyde, Glasgow, UK, with "Patrick D. Ritchie Prize" for the best Ph.D. in 1994. With more than a decade experience in large international incorporations, Prof. Pan has been engaged in fundamental research and product development of novel optoelectronic and energy storage materials and devices. As Chief Scientist, Prof. Pan led 8 entities in Shenzhen to win the 150 million RMB grant for the national new energy vehicles (power battery) innovation project from 2013 to end of 2015. As Chief Scientist, Prof. Pan led 12 entities to win National Key project of Material Genomic Engineering for Solid State Li-ion Battery in China in 2016.